JOURNAL OF CATALYSIS 113, 497–508 (1988)

# Alkyl Elimination from Aldehydes on Zinc Oxide: Relevance to Allylic Oxidation Pathways

J. M. VOHS AND M. A. BARTEAU[1]

*Center for Catalytic Science and Technology, Department of Chemical Engineering, University of Delaware, Newark, Delaware 19716*

Received January 6, 1988; revised April 26, 1988

The reactions of acetaldehyde, propionaldehyde, and acrolein on the (0001)-Zn polar surface of zinc oxide were investigated using temperature-programmed desorption and X-ray photoelectron spectroscopy. Oxidation of these aldehydes on the (0001)-Zn surface proceeded via two competing pathways: nucleophilic addition of lattice oxygen at the carbonyl carbon followed by hydride elimination to form the corresponding surface carboxylate species, and nucleophilic attack of lattice oxygen at the carbonyl carbon followed by alkyl elimination to form surface formate species. There was a strong temperature dependence of the selectivity toward these two competing pathways; low temperatures favored alkyl elimination, while high temperatures favored hydride elimination. The decomposition of the higher carboxylates resulted in the formation of both unsaturated carbonyl compounds and carbon oxides. The possible implications of these results for allylic oxidation reactions on metal oxide catalysts are discussed. © 1988 Academic Press, Inc.

## INTRODUCTION

The selective oxidation and ammoxidation of olefins over metal oxide or mixed metal oxide catalysts is practiced industrially for the production of aldehydes, nitriles, and carboxylic acids. Because of their industrial importance, the mechanisms of these allylic oxidations have been the subject of numerous investigations (*1–6*). In the case of propylene oxidation to acrolein, it is generally accepted that oxidation proceeds via the initial abstraction of a hydrogen $\alpha$ to the carbon–carbon double bond to form an allylic surface intermediate (*1–2*). This allylic intermediate reacts with lattice oxygen to form either alkoxide or carboxylate surface species. Decomposition of these oxygenated surface species ultimately leads to the formation of acrolein or acrylic acid. The ammoxidation reaction proceeds via a similar mechanism in which the allylic intermediate undergoes nitrogen insertion followed by hydrogen shift reactions to form acrylonitrile (*1, 2, 5*).

Although the mechanisms of the selective oxidation and ammoxidation reactions are relatively well understood, the unselective oxidation pathways which proceed either in parallel or in series with the selective pathways have received surprisingly little attention. Even on highly selective catalysts such as bismuth molybdates, carbon oxides and small amounts of formaldehyde, acetaldehyde, propionaldehyde, and acetone are produced by undesirable side reactions (*4, 7*). For propylene ammoxidation, HCN and $CH_3CN$ also appear as unwanted products along with the complete oxidation products, CO and $CO_2$ (*8*).

Davydov *et al.* (*9*) have used IR spectroscopy to identify the surface species formed during propylene oxidation to acrolein on several metal oxides, including supported molybdena, gallium molybdate, and copper and chromium oxides. These authors found that in addition to $\pi$-allyl and $\sigma$-allyl surface complexes, acetate, formate, and carbonate surface species were formed. The

---

[1] To whom correspondence should be addressed.

0021-9517/88 $3.00
Copyright © 1988 by Academic Press, Inc.
All rights of reproduction in any form reserved.

mechanisms leading to the formation of these surface species were not determined, but the authors postulated that the surface allyl species and the surface carboxylate species were produced by parallel reaction pathways. Decomposition of the surface carboxylate and carbonate intermediates was thought to lead to the formation of both complete oxidation products and saturated aldehydes. These results suggest that undesirable products can be formed via two general reaction pathways: the first, which can account for the complete oxidation products, is the overoxidation of the desired products to form carbon oxides; the second involves the parallel unselective activation of the olefin which leads to the formation of both carbon oxides and saturated aldehydes. It is also possible that unselective side reactions of the surface intermediates which are formed along the selective oxidation pathway may lead to undesirable products. The factors which control these unselective reaction pathways are not well understood.

Grasselli and co-workers have mapped out the network of reactions leading to selective oxidation of propylene with bismuth–molybdate catalysts by entering the network at different points via the judicious choice of model reactants (*1*, *2*, *6*). The application of this strategy to elucidate the mechanisms of potential side reactions requires an unselective oxide as well, since the best catalysts yield few of the undesired products. Like the bismuth–molybdate system, zinc oxide forms allylic intermediates via dissociative adsorption of propylene (*10–12*) and has been a common model material in studies of the interaction of allyls with oxides (*11–13*). However, the subsequent reactions of surface allyls on zinc oxide are essentially unselective (*13*). We report here studies of aldehyde oxidation on the Zn-polar face of zinc oxide. These studies provide evidence for previously unrecognized reactions which may limit the selectivity of oxide-catalyzed reactions involving carbonyl compounds as reactants, intermediates, or products. We also report evidence for a second route to acrolein via adsorbed propionate intermediates. While some caution is required in generalizing these reactions to other oxides, we note published evidence, both direct and circumstantial, for analogous chemistry on a range of materials which includes molybdate-based catalysts.

## EXPERIMENTAL

All experiments were conducted in a conventional ultrahigh-vacuum chamber which has been described previously in detail (*14*, *15*). The chamber was equipped with a cylindrical mirror analyzer and electron and X-ray sources for performing AES and XPS. The chamber was also equipped with a quadrupole mass spectrometer for collection of TPD spectra. The mass spectrometer was multiplexed with an IBM personal computer. The computer was also used to control the heating rate during TPD experiments.

The zinc oxide single crystal used in this investigation was obtained from Litton Airtron and was aligned normal to the *C*-axis using the Laue method. The crystal mounting and cleaning procedures were identical to those used previously (*14*, *15*).

All XPS spectra were collected using Al$K\alpha$ X-rays (1486.6 eV). Small band-bending shifts (less than 0.4 eV) were observed following adsorption of the aldehydes on the (0001)-Zn surface. In order to account for these band-bending shifts all XPS spectra were referenced as in previous studies (*14*–17) to the Zn($2p_{3/2}$) peak at 1021.7 eV on the clean surface.

Acetaldehyde (Aldrich, 99%), propionaldehyde (Alfa, 99%), acrolein (Aldrich, 97%), and propionic acid (Aldrich, 99%), were purified by repeated freeze–pump–thaw cycles prior to use. They were admitted into the vacuum chamber through dosing needles pointed toward the front face of the crystal. Saturation coverages were used in all experiments. With an enhancement of the flux to the crystal by a

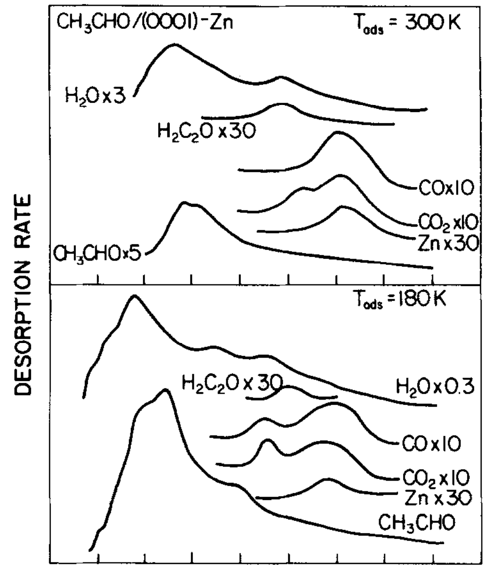

FIG. 1. Temperature-programmed desorption spectra following $CH_3CHO$ adsorption on ZnO(0001): upper half, $T_{ads}$ = 300 K; lower half, $T_{ads}$ = 180 K.

factor of 25 from the dosing needle, a 50-Langmuir dose was found to be sufficient to saturate the surface with the organic reactants used in this study.

## RESULTS

TPD spectra following adsorption of acetaldehyde on the (0001)-Zn polar surface at 300 K are displayed in Fig. 1. The relative product yields are listed in Table 1. The major decomposition products were $H_2C_2O$ (ketene) and $H_2O$ which desorbed at 590 K, $CO_2$ which exhibited peaks at 640 and 710 K, and CO and Zn which also desorbed at 710 K.

The TPD spectra displayed in Fig. 1 were similar to those observed previously for the decomposition of acetic acid on the (0001)-Zn surface (*17*). This similarity suggests that the same surface species were formed from both reactants. XPS and UPS results have clearly demonstrated that surface acetate species are formed from acetic acid on the Zn-polar surface (*17*). Surface acetate species could also be formed from acetaldehyde via nucleophilic attack of lattice oxygen at the carbonyl carbon and subsequent hydride elimination. Analogous nucelophilic reactions have been observed previously for both formaldehyde (*14*) and methyl formate (*16*) on the (0001)-Zn surface; for these molecules nucleophilic attack by lattice oxygen resulted in the formation of surface formate species.

TPD spectra obtained following the adsorption of propionaldehyde on the (0001)-Zn surface at 300 K are displayed in Fig. 2. The relative product yields are listed in Table 2. For comparison, TPD spectra from the $CH_3CH_2COOH$-dosed (0001)-Zn surface (*17*) are displayed in Fig. 3. The TPD spectra for the $CH_3CH_2CHO$- and $CH_3CH_2COOH$-dosed surfaces were similar, again suggesting that $CH_3CH_2CHO$, like $CH_3CH_2COOH$, decomposed via surface propionate species on the (0001)-Zn surface. The principal difference between the two sets of spectra was the absence of acrolein as a decomposition product from $CH_3CH_2CHO$. Acrolein was not observed from the (0001)-Zn surface for $CH_3CH_2CHO$ adsorption temperatures between 180

TABLE 1

Desorption Products from the $CH_3CHO$-Dosed (0001)-Zn Surface

| | Product | Peak temperature (K) | Relative yield[a] |
|---|---|---|---|
| $T_{ads}$ = 300 K | $H_2C_2O$ | 590 | 0.17 |
| | $H_2O$ | 590 | 0.45 |
| | $CO_2$ | 640 | 0.46 |
| | $CO_2$ | 710 | 1.00 |
| | CO | 710 | 0.82 |
| | Zn | 710 | 0.56 |
| $T_{ads}$ = 180 K | $H_2O$ | 560 | 2.49 |
| | $CO_2$ | 560 | 0.73 |
| | CO | 560 | 0.54 |
| | $H_2C_2O$ | 600 | 0.21 |
| | $CO_2$ | 680 | 2.06 |
| | CO | 680 | 1.80 |
| | Zn | 680 | 0.85 |

[a] Corrected for mass spectrometer sensitivities.

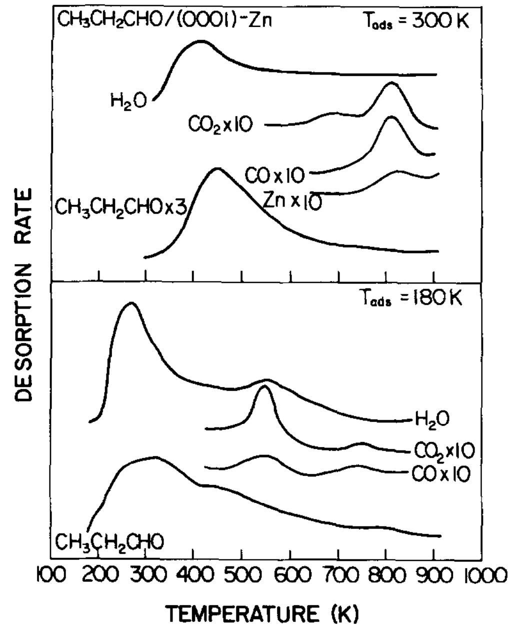

FIG. 2. Temperature-programmed desorption spectra following $CH_3CH_2CHO$ adsorption on ZnO(0001): upper half, $T_{ads}$ = 300 K; lower half $T_{ads}$ 180 K.

TABLE 2

Desorption Products from the $CH_3CH_2CHO$-Dosed (0001)–Zn Surface

| | Product | Peak temperature (K) | Relative yield[a] |
|---|---|---|---|
| $T_{ads}$ = 300 K | $CO_2$ | 685 | 0.38 |
| | $CO_2$ | 815 | 1.00 |
| | CO | 815 | 0.70 |
| | Zn | 815 | 1.07 |
| $T_{ads}$ = 180 K | $CO_2$ | 560 | 0.95 |
| | CO | 560 | 0.34 |
| | $H_2O$ | 560 | 1.92 |
| | $CO_2$ | 740 | 0.14 |
| | CO | 740 | 0.13 |

[a] Corrected for mass spectrometer sensitivities.

and 330 K; in contrast, acrolein, which desorbed at 620 K, was a major decomposition product for propionic acid. Following propionaldehyde adsorption at 300 K, the major decomposition products were $H_2O$, which desorbed in a low-temperature peak centered at 405 K, CO and Zn which desorbed at 815 K, and $CO_2$ which desorbed at both 685 and 815 K.

Variations in the aldehyde adsorption temperature resulted in significant changes in both the relative yields and the peak temperatures for the products from both $CH_3CHO$ and $CH_3CH_2CHO$. Reduction of the dosing temperature resulted in a decrease in the intensity of the high-temperature CO, $CO_2$, and Zn peaks for both reactants. For dosing temperatures below ca. 240 K, a new set of carbon oxide peaks centered between 500 and 600 K was ob-

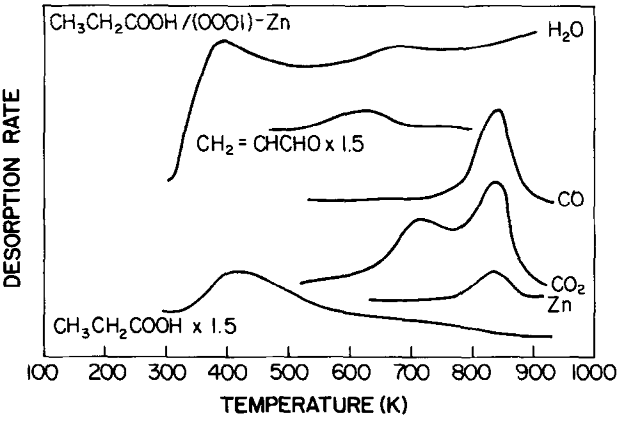

FIG. 3. Temperature-programmed desorption spectra following $CH_3CH_2COOH$ adsorption on ZnO(0001) at 300 K.

served in addition to the high-temperature carbon oxide products.

TPD spectra following adsorption of $CH_3CHO$ on the (0001)-Zn surface at 180 K are displayed in Fig. 1. The relative yields of the major decomposition products are listed in Table 1. The high-temperature carbon oxide peaks were at slightly lower temperatures than those observed for $T_{ads} = 300$ K, and only a single $CO_2$ peak was observed above 600 K. The high-temperature CO and $CO_2$ peaks were very broad, suggesting that they were composed of several overlapping peaks. A small $H_2C_2O$ peak was evident at 600 K, in the same position as that following adsorption at higher temperatures. In addition to these products, CO, $CO_2$ and $H_2O$ peaks centered at 560 K were observed. As noted above, these low-temperature oxidation products appeared only for adsorption temperatures less than 240 K.

The changes in the TPD spectra for the $CH_3CH_2CHO$-dosed (0001)-Zn surface with decreasing adsorption temperature were more dramatic than those for the $CH_3CHO$-dosed surface. TPD spectra obtained following $CH_3CH_2CHO$ adsorption at 180 K are displayed in Fig. 2, and the relative product yields are listed in Table 2. In contrast to the results obtained for $T_{ads} =$ 300 K, only small amounts of carbon oxide products were detected above 600 K. The major decomposition products were CO, $CO_2$ and $H_2O$ which desorbed at 560 K, i.e., the same temperature as the low-temperature carbon oxide products from $CH_3CHO$.

The decomposition of acrolein on the (0001)-Zn surface displayed trends analogous to those for acetaldehyde and propionaldehyde. Following adsorption at 300 K the primary decomposition products, CO, $CO_2$, $H_2O$, and $H_2$, desorbed at 760 K, while following adsorption at 155 K, small CO and $CO_2$ peaks were also evident at 560 K. The CO and $CO_2$ desorption spectra for the acrolein-dosed surface for these two adsorption temperatures are displayed in Fig. 4. The overall yield of lower-temperature carbon oxides from acrolein was substantially less than that observed for the other aldehydes. The observation of carbon oxides at ca. 560 K common to the reaction of all three aldehydes suggests that these products are characteristic of the reaction of aldehydes on the (0001)-Zn surface at low temperatures.

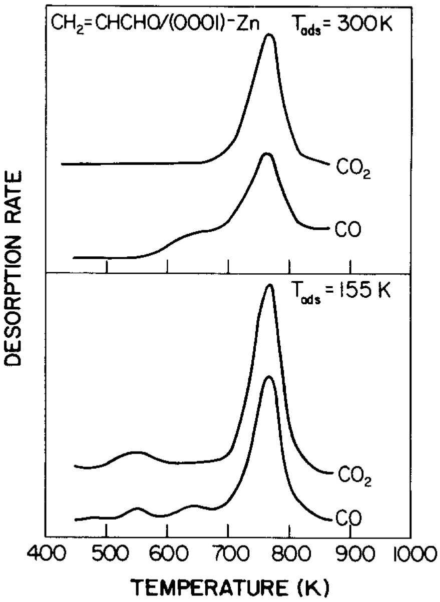

FIG. 4. Temperature-programmed desorption spectra for CO and $CO_2$ following $CH_2$ = CHCHO adsorption on ZnO(0001): upper half, $T_{ads} = 300$ K; lower half $T_{ads} = 155$ K.

The low-temperature CO, $CO_2$, and $H_2O$ peaks produced from these higher aldehydes for adsorption temperatures below 240 K were quite similar to those for the decomposition of formate species on the Zn-polar surface of ZnO (*14, 16–20*). For example, surface formates produced from formic acid were shown to decompose at 575 K to produce primarily CO, $CO_2$, $H_2$, and $H_2O$. This similarity of the decomposition behavior suggests that surface formate species are also produced by reaction of the aldehydes at low temperature on the (0001)-Zn surface. The production of formate species via oxidation of higher aldehydes is a surprising result and would appear to indicate that the initial nucleo-

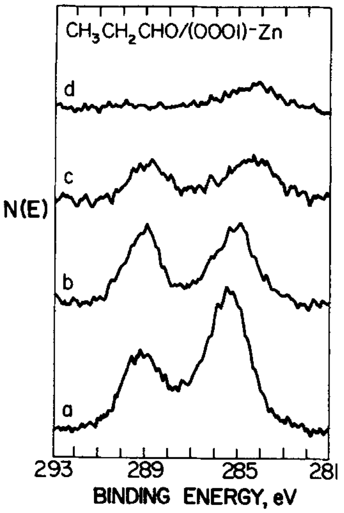

FIG. 5. C(1*s*) XPS spectra of the $CH_3CH_2CHO$-dosed (0001)-Zn surface as a function of sample temperature. (a) $CH_3CH_2CHO$-dosed (0001)-Zn surface at 170 K. (b) Sample in (a) heated to 300 K. (c) Sample in (b) heated to 450 K. (d) Sample in (c) heated to 600 K.

philic attack of lattice oxygen at the carbonyl carbon of the aldehydes is accompanied by carbon–carbon bond cleavage and elimination of the alkyl group. Unfortunately, since only carbon oxide products of this reaction were observed to desorb, the identification of the various surface intermediates based on the TPD results alone is somewhat hazardous. Therefore, in an effort to further characterize the surface species produced via reaction of the aldehydes on the (0001)-Zn surface, C(1*s*) photoelectron spectra of the adsorbed species were obtained.

C(1*s*) spectra of the $CH_3CH_2CHO$-dosed (0001)-Zn surface following adsorption at 170 K are displayed in Fig. 5. At 170 K the spectrum (curve a, Fig. 5) consisted of two overlapping peaks centered at 285.4 and 289.0 eV. These peaks were in positions similar to those of surface propionate species formed from propionic acid on this surface (*17*). By analogy with these results, the two peaks observed at 285.4 and 289.0 eV following $CH_3CH_2CHO$ adsorption at 170 K can be assigned the alkyl group carbon and to a carbon bound to two oxygens, respectively. The 3.6-eV separation of these two peaks is approximately 1 eV greater than that typically observed between the carbonyl and the alkyl carbons in gaseous aldehydes (*21*). This further supports the assignment of the high binding-energy peak to a carbon bound to two oxygens. Thus, these results demonstrate the nucleophilic attack of lattice oxygen at the carbonyl carbon of the aldehyde. This results in the formation of a di-oxy alkylidene surface species; a subsequent elimination reaction would lead to the formation of surface carboxylate species.

Heating the $CH_3CH_2CHO$-dosed surface to 300 K produced significant changes in the C(1*s*) spectrum (curve b, Figure 5). At 300 K the spectrum consisted of two peaks centered at 285.1 and 289.0 eV. The shift in the position of the low binding-energy peak relative to that at 170 K was most likely a result of the loss of molecularly adsorbed species from the surface. The valley between the two peaks extended nearly to the baseline in the spectrum at 300 K, while at 170 K the valley was substantially above the baseline. This observation is also consistent with the loss of molecular species from the surface, since the carbonyl carbon of molecularly adsorbed propionaldehyde would occur between the two major peaks of the surface carboxylate or di-oxy species. The carboxylate/alkyl C(1*s*) peak area ratio observed at 300 K was 0.68. This ratio is slightly greater than the maximum ratio of 0.5 expected for surface propionate species. The ratio for propionates produced from propionic acid, 0.3, was even lower due to screening of the surface-bound carboxylate carbon by the alkyl group (*17*). The higher-than-expected peak area ratio is consistent with the TPD results and suggests that other intermediates in addition to surface propionate species were formed following the adsorption of $CH_3CH_2CHO$ on the (0001)-Zn surface at 170 K. The TPD results indicated the formation of both propionate and formate species. Formates adsorbed on the (0001)-Zn surface exhibit a C(1*s*) binding energy of 289.1 eV (*14*, *16*), nearly the same as that observed for the carboxylate carbon of absorbed propionates (*17*). The formation of both formates and propionates from propionaldehyde would tend to increase the area of the higher binding-energy carboxylate carbon peak relative to the lower binding-energy alkyl carbon peak. This is exactly the trend in the C(1*s*) spectra displayed in Fig. 5. Thus, the XPS results support the conclusion that both propionate and formate species were formed by reaction of propionaldehyde on the (0001)-Zn surface at low temperature.

Heating the $CH_3CH_2CHO$-dosed surface to 450 K caused significant broadening of the low binding-energy peak, indicative of the formation of a new carbon species at higher temperatures. Curve resolution of the spectra determined that this new surface species gave rise to a peak centered at 284.0 eV. This peak position is close to that at which peaks from adsorbed atomic carbon are commonly observed on this surface (*15*, *17*). Therefore, this new peak may be due to the deposition of atomic carbon during the reactions of aldehydes. Zinc alkyls also exhibit low C(1*s*) binding energies (*21*). For example, diethylzinc adsorbed on the (0001)-Zn surface exhibits two C(1*s*) peaks centered at 283.4 and 284.6 eV (*22*). Thus, this peak may also be due to the formation of surface zinc alkyl species. Since alkyl elimination from adsorbed aldehydes or di-oxy alkylidene complexes would deposit alkyl groups on the surface, this explanation is also consistent with the formation of formates from the aldehydes. These surface alkyls would most likely be coordinated to surface zinc cations.

Further heating of the surface to 600 K resulted in a single peak centered at 284.0 eV. Again this peak is most likely due to adsorbed atomic carbon, surface zinc alkyl species, or a combination of the two. Heating to temperatures above 800 K was sufficient to produce a carbon-free surface.

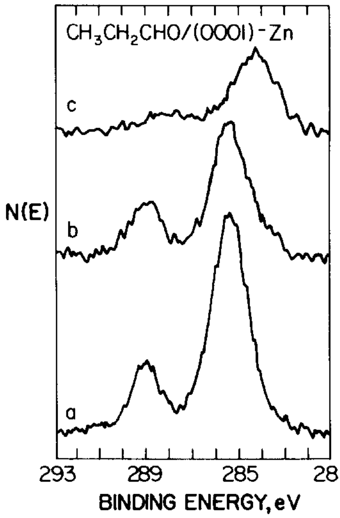

FIG. 6. C(1*s*) XPS spectra of the $CH_3CH_2CHO$-dosed (0001)-Zn surface as a function of sample temperature. (a) $CH_3CH_2CHO$-dosed (0001)-Zn surface at 300 K. (b) Sample in (a) heated to 450 K. (c) Sample in (b) heated to 600 K.

C(1*s*) spectra of the $CH_3CH_2CHO$-dosed surface following adsorption at 300 K (Fig. 6) were qualitatively similar to those obtained for $T_{ads}$ = 170 K, except that the ratios of the areas of the carboxylate peaks to those of the alkyl peaks were significantly less than those observed for the lower adsorption temperatures. Spectra were also obtained following $CH_3CH_2CHO$ adsorption at 240 K. The ratios of the carboxylate/alkyl C(1*s*) peak areas as a function of surface temperature for the three $CH_3CH_2CHO$ dosing temperatures are displayed in Fig. 7. The data in Fig. 7 clearly demonstrate that an increase in the adsorption temperature results in a decrease in the carboxylate/alkyl C(1*s*) peak area ratio. The ratios obtained following heating of the surface in each case to 450 K are particularly interesting, since the TPD results indicated that for this sample temperature no molecularly adsorbed aldehydes were present on the surface. Thus, the ratios at 450 K reflect the true ratio of carboxylate to alkyl carbons contained in surface intermediates. At lower temperatures the presence of small amounts of

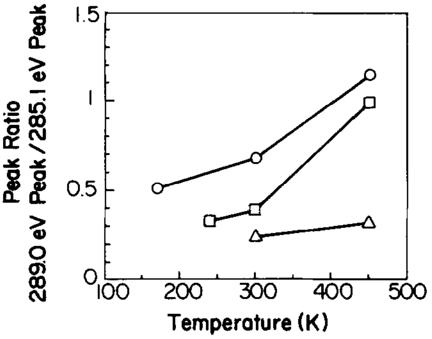

FIG. 7. Carboxylate/alkyl C(1*s*) peak area ratio for the $CH_3CH_2CHO$-dosed (0001)-Zn surface as a function of sample temperature: (○) $T_{ads}$ = 170 K, (□) $T_{ads}$ = 240 K, and (△) $T_{ads}$ = 300 K.

molecularly adsorbed propionaldehyde tends to decrease the observed ratio, since the molecular species C(1*s*) binding energies overlap with those of the alkyl carbons of surface carboxylate species. The carboxylate/alkyl peak area ratio for experiments in which the surface was dosed at 300 K and then heated to 450 K was 0.32. This ratio was substantially less than the expected ratio of 0.5 for surface propionate species. Photoelectron spectra of surface carboxylate species adsorbed on the (0001)-Zn surface obtained recently (*17*) have demonstrated, however, that substantial shielding of the surface-bound carboxylate carbon by the alkyl carbons occurs, resulting in lower-than-expected peak areas ratios. For example, surface acetates adsorbed on the (0001)-Zn surface have a carboxylate/alkyl C(1*s*) peak area ratio of 0.8, while for surface propionates this ratio is 0.3. Thus, the ratio observed for the $CH_3CH_2CHO$-dosed surface following adsorption at 300 K and heating to 450 K was almost identical to that reported previously for surface propionate species. This result is consistent with the TPD results and further demonstrates that only surface propionates were formed from propionaldehyde following adsorption at temperatures greater than 300 K.

Carboxylate/alkyl C(1*s*) peak area ratios substantially greater than those observed for an adsorption temperature of 300 K were observed following $CH_3CH_2CHO$ adsorption at both 170 and 240 K followed by heating to 450 K. For $T_{ads}$ = 170 K the ratio was 1.15, while for $T_{ads}$ = 240 K the ratio was 0.99. These values are more than three times that for surface propionate species alone and clearly demonstrate that intermediates in addition to propionates were present on the surface following adsorption at these temperatures. As described above, this result is consistent with TPD results and further demonstrates that both propionate and formate species were produced during the reaction of propionaldehyde on the (0001)-Zn surface at temperatures below 240 K.

XPS spectra of the $CH_3CHO$-dosed surface exhibited trends similar to those for the $CH_3CH_2CHO$-dosed (0001)-Zn surface. Following adsorption at 450 K the ratio of the carboxylate carbon peak area to that of the alkyl carbon peak was 0.75, while following adsorption at 170 K and heating to 450 K the peak area ratio was 0.92. This is again consistent with the TPD results and supports the formation of surface formate species from acetaldehyde at low temperatures.

## DISCUSSION

The results obtained in this investigation may have important implications for selective oxidation of hydrocarbons on metal oxide catalysts. The alkyl elimination pathway which led to the formation of surface formate species during the reaction of aldehydes on the (0001)-Zn surface represents a low-temperature pathway that ultimately results in the formation of both complete oxidation products and undesired selective oxidation products. Similar pathways in the case of propylene ammoxidation may be able to account for the low-temperature formation of HCN and $CH_3CN$.

The reaction network for the conversion of propionaldehyde and propionic acid on the (0001)-Zn surface is summarized in Fig.

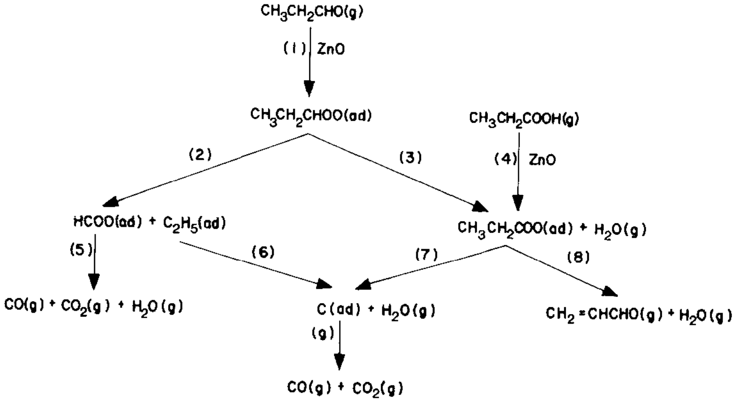

FIG. 8. Reaction pathways for the decomposition of $CH_3CH_2CHO$ and $CH_3CH_2COOH$ on ZnO(0001).

8. As discussed previously (*17*), $CH_3CH_2COOH$ adsorbed dissociatively on the (0001)-Zn surface at temperatures between 180 and 450 K to form surface propionate species (step 4 in Fig. 8). Adsorbed propionaldehyde reacted with lattice oxygen on the (0001)-Zn surface to form surface propionate species for adsorption temperatures between 150 and 330 K (steps 1 and 3 in Fig. 8). However, a second competing reaction pathway was also observed: both the TPD and the XPS results demonstrated that this second pathway resulted in the formation of surface formate species (steps 1 and 2 in Fig. 8). The selectivity for these two competing reaction pathways showed a strong temperature dependence. Following aldehyde adsorption at 300 K only the pathway leading to the corresponding carboxylate species was observed. For this adsorption temperature, the TPD results were similar to those for propionic acid and characteristic of the decomposition of surface propionate species. In contrast to adsorption at 300 K, propionaldehyde adsorption at temperatures below ca. 240 K resulted in TPD products characteristic of the decomposition of both surface formate and the higher carboxylate species.

Although both the carboxylic acids and the aldehydes reacted on the (0001)-Zn surface to form the corresponding surface carboxylate species, the selectivity for their decomposition (steps 6 and 7 in Fig. 8) was found to be dependent on the origin of the carboxylates. Carboxylates produced from the carboxylic acids exhibited a high selectivity for reaction to unsaturated aldehydes, while carboxylates produced from the aldehydes had a high selectivity for oxidation to CO and $CO_2$. For example, on the carboxylic acid-dosed surfaces the ratio of the fraction of surface carboxylate species which decomposed to unsaturated aldehydes to that which was completely oxidized was 1.5 for acetates and 0.75 for propionates (*17*). For acetates produced via reaction of acetaldehyde on the (0001)-Zn surface at 300 K, the corresponding ratio was 0.2, while for the propionates produced from propionaldehyde no unsaturated aldehydes were detected as decomposition products.

Since the XPS results did not provide any evidence which would suggest chemical differences between the higher carboxylates produced from the aldehydes and those produced from the carboxylic acids, it is somewhat surprising that there was such a large difference in selectivity for the decomposition of these carboxylates. It is possible that these differences in selectivity were due in part to differences in the extent of reduction of the surface produced by reaction of the carboxylic acids and the aldehydes. Since the formation of carboxylates from the aldehydes requires lattice oxygen, carboxylate species produced from the aldehydes may be bound to a more reduced surface than those produced from the carboxylic acids. This difference in the extent of surface reduction may result in changes in the selectivity.

It is also possible that differences in the coordination of the surface carboxylate species produced from the aldehydes and carboxylic acids account for the differences in carboxylate decomposition selectivity. As suggested previously, dissociative adsorption of the carboxylic acids may favor the formation of monodentate carboxylates while reaction of the aldehydes may favor formation of bidentate carboxylates (*17*). The decomposition of monodentate carboxylates would be expected to favor aldehyde production, while decomposition of bidentate carboxylates would favor the unselective decomposition products. Recent results for the decomposition of monodentate and bidentate acetates on platinum surfaces (*23*) have displayed such trends in selectivity.

Even more surprising than the differences in selectivity for higher carboxylate decomposition between the aldehyde and the carboxylic acid-dosed surfaces was the appearance of formate decomposition products following the adsorption of acetaldehyde, propionaldehyde, and acrolein on the (0001)-Zn surface at low temperatures. The production of formate species from the aldehydes requires carbon–carbon bond cleavage and elimination of the alkyl group from the aldehyde. This reaction provides a low-temperature pathway to the formation of unselective oxidation products and may limit the overall selectivity obtainable with metal oxide catalysts. The mechanism by which this alkyl elimination occurs is not clear; however, comparisons of the TPD results for the aldehydes and carboxylic acids may provide insight into possible reaction pathways.

Since alkyl elimination was observed only for the aldehydes and not for the carboxylic acids, low-temperature alkyl elimination must occur prior to carboxylate formation. The initial reaction of the aldehydes with the surface is undoubtedly nucelophilic attack via lattice oxygen at the carbonyl carbon of the aldehyde to form a di-oxy alkylidene surface species (step 1, Fig. 8). Subsequent elimination reactions lead to the formation of formate or the higher carboxylate depending on whether the hydride or the alkyl group is eliminated. These reactions can be considered to be analogous to well-known nucleophilic addition–displacement reactions commonly observed in solution. In the case of the surface reactions, lattice oxygen acts as the nucleophile; the alkyl group and the hydrogen atom act as leaving groups. In solution a hydrogen atom, almost without exception, is a better leaving group than an alkyl group. Thus, nucleophilic addition–displacement reactions of aldehydes in solution proceed via hydride elimination rather than alkyl group eliminations. Although the solution chemistry is complicated by effects of solvation which are not present for gas–solid reactions, this observation suggests that alkyl elimination reactions of aldehydes may be a novel property of the surface chemistry of metal oxides. Indeed, the formation of surface formate species during the oxidation of aldehydes and ketones has been observed on several metal oxides, including MgO and NiO (*24*), in addition to ZnO (*25*).

The strong temperature dependence of the relative rates of alkyl elimination and hydride elimination indicates that hydride elimination is a more highly activated process than alkyl group elimination on zinc oxide. Thermochemical calculations predict that the $\alpha$ C–H bond energy in propionaldehyde is approximately 13 kcal/mol greater than the $\alpha$ C–C bond energy (*26*, *27*). Therefore, the temperature dependence of the reaction of aldehydes on the (0001)-Zn surface may simply reflect these differences in the $\alpha$ C–H and $\alpha$ C–C bond energies of the aldehydes. The ratio of the rate of hydride elimination to that of alkyl elimination can be estimated from the ratio of the coverage of surface formates and propionates produced for each dosing temperature. The relative coverage of formates and propionates produced from propionaldehyde following adsorption at 170 K, as determined from the C(1*s*) peak areas, was approximately 1.7. For adsorption at 300 K, both the XPS and the TPD results indicated that the rate of hydride elimination was at least 10 times greater than the rate of alkyl elimination. These two relative rates yield an activation energy difference between the two pathways of 9.2 kcal/mol, in reasonable agreement with the 13 kcal/mol difference in $\alpha$ C–H and $\alpha$ C–C bond energies for propionaldehyde.

Differences in bond energies may also be able to explain the differences in the relative coverages of formate species produced from the three aldehydes. The TPD data demonstrated that for a fixed adsorption temperature the relative rates of formate formation to higher carboxylate formation increased in the order $CH_2 = CHCHO < CH_3CHO < CH_3CH_2CHO$. Although the $\alpha$ C–H bond energies do not vary significantly between the three aldehydes, there are significant variations in the $\alpha$ C–C bond energies. Thermochemical calculations yield $\alpha$ C–C bond energies for acrolein, acetaldehyde, and propionaldehyde of 87.5, 84.6, and 84.3 kcal/mol, respectively (*26*). Based on these bond energies one would predict the same order of relative rates of formate formation to higher carboxylate formation for the three aldehydes as was observed experimentally.

The results of this investigation suggest a possible route for production of surface formate and acetate species during the reaction of propylene on metal oxide surfaces via the reaction of the aldehyde selective oxidation products with lattice oxygen. This pathway is an alternative to the suggestion of Davydov *et al.* (*9*) that carboxylate species and $\pi$-allyl species are produced by parallel reactions of the adsorbed olefin. Although the selective oxidation pathways to produce unsaturated aldehydes appear to be similar on many metal oxides, the subsequent oxidation of the product aldehydes to produce carboxylate species appears to depend strongly on the nature of the interaction of the aldehyde with the metal oxide. On highly selective catalysts such as bismuth molybdates, aldehydes apparently do not react with surface oxygen to form carboxylate species (*4*). The formation of carboxylate species from aldehydes also appears to be important in the catalytic oxidation of propylene to produce acrylic acid. Highly selective bismuth–molybdate catalysts produce essentially no acrylic acid from propylene. Less selective catalysts such as tin molybdates and cobalt molybdates produce significant amounts of both acrolein and acrylic acid from propylene, suggesting that the aldehydes react to form higher carboxylate species on these surfaces (*4*). On even less selective catalysts such as zinc oxide, the reaction of aldehydes results in the formation of both formate and higher carboxylate species. The formation of formate species provides a low-temperature pathway to complete oxidation products, contributing to the low selectivity of zinc oxide as an olefin oxidation catalyst.

In addition to the observation of a low-temperature unselective aldehyde oxidation pathway, the behavior observed for the decomposition of the higher carboxylate species may also be relevant to selective oxidation of hydrocarbons on metal oxide catalysts. The decomposition of surface propionate species from propionic acid resulted in the production of acrolein. Thus, the decomposition of surface carboxylate species appears to provide an alternate pathway for the production of unsaturated aldehydes on metal oxide surfaces. Similar results were also obtained for the decomposition of surface acetates from both acetic acid and acetaldehyde; acetate decomposition produced ketene. In a recent study of carboxylic acid decomposition on $TiO_2$, unsaturated aldehydes were observed as decomposition products for both surface acetates and propionates (*28*). Thus, this route to unsaturated aldehydes may also be characteristic of metal oxides.

## CONCLUSIONS

Acetaldehyde, propionaldehyde, and acrolein underwent nucleophilic attack by lattice oxygen on the (0001)-Zn surface of ZnO followed by elimination of either the hydride or the alkyl group to form the corresponding surface carboxylate species and surface formate species, respectively. The alkyl elimination pathway was favored by adsorption by low temperatures, while adsorption at room temperature and above favored hydride elimination. The activation energy difference between these two competing pathways was found to correlate well with the differences in $\alpha$ C–H and $\alpha$ C–C bond dissociation energies for these aldehydes.

These results may have implications for selective oxidation of hydrocarbons by metal oxide catalysts. Alkyl elimination to produce surface formate species represents a low-temperature pathway that results in the formation of both complete oxidation products and undesired selective oxidation products. In the case of propylene ammoxidation, the analogous pathway may be able to account for the low-temperature formation of HCN and $CH_3CN$. The decomposition of surface carboxylate species may also provide an alternative to allylic oxidation pathways for the production of unsaturated aldehydes on metal oxide surfaces.

## ACKNOWLEDGMENTS

We gratefully acknowledge the support of the National Science Foundation (Grant CBT 8311912) and of E. I. du Pont de Nemours and Co., Inc.

## REFERENCES

*1.* Grasselli, R. K., and Burrington, J. D., *in* "Advances in Catalysis" (D. D. Eley, H. Pines, and P. B. Weisz, Eds.), Vol. 30, p. 133. Academic Press, New York, 1981.

*2.* Grasselli, R. K., *in* "Adsorption and Catalysis on Oxide Surfaces" (M. Che, and G. C. Bond, Eds.), p. 275. Elsevier, Amsterdam, 1985.

*3.* Voge, H. H., and Adams, C. R., *in* "Advances in Catalysis" (D. D. Eley, H. Pines, and P. B. Weisz, Eds.), Vol. 17, p. 151. Academic Press, New York, 1967.

*4.* Margolis, L. Ya., *Catal. Rev.* **8,** 241 (1974).

*5.* Adams, C. R., and Jennings, T. J., *J. Catal.* **2,** 63 (1963).

*6.* Burrington, J. D., and Grasselli, R. K., *J. Catal.* **87,** 363 (1984).

*7.* Keulks, G. W., Krenzke, L. D., and Notermann T. N., *in* " Advances in Catalysis" (D. D. Eley, H. Pines, and P. B. Weisz, Eds.), Vol. 27, p. 183. Academic Press, New York, 1978.

*8.* Zhdan, P. A., Shepelin, A. P., Osipova, Z. G., and Sokolovskii, V. I., *J. Catal.* **58,** 363 (1984).

*9.* Davydov, A. A., Mikhaltchenko, V. G., Sokolovskii, V. D., and Boreskov, G. K., *J. Catal.* **55,** 8 (1979).

*10.* Dent, A. L., and Kokes, R. J., *J. Amer. Chem. Soc.* **92,** 6709 (1970).

*11.* Kokes, R. J., *Intra-Sci. Chem. Rep* **6,** 77 (1972).

*12.* Hata, K., Kawasaki, S., Kubokawa, Y., and Miyata, H., *in* "Proceedings, Sixth International Congress on Catalysis" (G. C. Bond, P. B. Wells, and F. C. Tompkins, Eds.), p. 1102. The Chemical Society, London, 1976.

*13.* Davydov, A. A., Yefremov, A. A., Mikhaltchenko, V. G., and Sokolovskii, V. D., *J. Catal.* **58,** 1 (1979).

*14.* Vohs, J. M., and Barteau, M. A., *Surf. Sci.* **176,** 91 (1986).

*15.* Vohs, J. M., and Barteau, M. A., *J. Phys. Chem.* **91,** 4766 (1987).

*16.* Vohs, J. M., and Barteau, M. A., *Surf. Sci.* **197,** 109 (1988).

*17.* Vohs, J. M., and Barteau, M. A., *Surf. Sci.*, in press.

*18.* Akhter, S., Lui, K., and Kung, H. H., *J. Phys. Chem.* **89,** 1958 (1985).

*19.* Lui, K., Vest, M., Berlowitz, P., Akhter, S., and Kung, H. H., *J. Phys. Chem.* **90,** 3183 (1986).

*20.* Zwicker, G., Jacobi, K., and Cunningham, J., *Int. J. Mass. Spectrom. Ion Processes* **60,** 213 (1984).

*21.* Bakke, A. A., Chen, H.-W., and Jolly, W. L., *J. Electron Spectrosc. Relat. Phenom.* **20,** 333 (1980).

*22.* Vohs, J. M., Ph.D. dissertation, University of Delaware, 1988.

*23.* Vajo, J. J., Sun, Y.-K., and Weinberg, W. H., *J. Phys. Chem.* **91,** 1153 (1987).

*24.* Miyata, H., Wakamiya, M., and Kubokawa, Y., *J. Catal.* **34,** 117 (1974).

*25.* Miyata, H., Hata, K., and Kubokawa, Y., *J. Catal.* **49,** 8 (1977).

*26.* Sanderson, R. T., "Chemical Bonds and Bond Energies." Academic Press, New York, 1971.

*27.* Benson, S. W., "Thermochemical Kinetics," Wiley, New York, 1968.

*28.* Kim, K. S., and Barteau, M. A., *Langmuir* **4,** in press (1988).